

**METIS Visible light relay  
optics concept and design**

Crescenzo, Giuseppe; Capobianco,  
Gerardo; Fineschi, Silvano



## DOCUMENT CHANGE RECORD

DATE	DESCRIPTION OF CHANGE	BY	APPROVED BY
07/12/2010	1 <sup>st</sup> Draft	G. Crescenzo	S.Fineschi

## Summary

<b>DOCUMENT CHANGE RECORD</b>	<b>2</b>
<b>Summary</b>	<b>3</b>
<b>Index of figure</b>	<b>4</b>
<b>Visible-light path and polarimeter</b>	<b>5</b>
<b>Constrains</b>	<b>5</b>
<b>Physical Limit</b>	<b>5</b>
<b>LCVR Polarimeter Constrains</b>	<b>6</b>
Acceptance angle	7
Footprint	7
VL folding mirror “instrument polarization”	7
Cross-Talk Polarization	8
<b>Envelope</b>	<b>10</b>
<b>Glass</b>	<b>10</b>
<b>Mass budget</b>	<b>10</b>
<b>Optical performances</b>	<b>11</b>
<b>LCVR design</b>	<b>12</b>
Baseline Vs BackVL Path	13
<b>Back up HW design</b>	<b>14</b>
Baseline Vs Back VL Path	15
<b>List of Acronyms</b>	<b>16</b>
<b><i>References</i></b>	<b>16</b>

## Index of figure

<b>Figure 1</b> The 2 focal planes UV and VL of METIS .....	5
<b>Figure 2</b> Schematic diagram of a lens with object and image planes, entrance and exit pupils, and marginal and chief rays. The entrance pupil is located at E and the exit pupil at E'. The chief ray passes through the edges of the fields and the centers of the pupils. The marginal ray passes through the axial object and image points and the edges of the pupils (from Handbook of Optics, McGraw-Hill) .....	6
<b>Figure 3</b> The LCVR devices and its parts, the ray comes from the farer fields at $\pm 3^\circ$ and are collimated in a cone of $\pm 3^\circ$ .....	6
<b>Figure 4</b> On the left (a) the first part of the VL path, the beam is "stretched" to create on the LCVR plane (b) a superposition of all the fields to minimize effects due to a non uniformity in the LC. ....	7
<b>Figure 5</b> The blue dots represents the polarization introduce by a multi layer MgF2 & Al folding mirror in function of the incidence angle, the red dots for MgF2 and Ag. The lines are the fits relative to the two series, the relation is quadratic. ....	8
<b>Figure 6</b> ZEMAX polarization pupil maps in the METIS VL focal plane. The boxes are for 3 position of the FM . In the last (bottom dx corner) a zoom show the visible change in polarization state. ....	9
<b>Figure 7</b> A draw of METIS envelope, the green area represents the space for the VL path location. ....	10
<b>Figure 8</b> Comparison between different FM angles. In the range between $30^\circ$ and $18^\circ$ (i.e. $25^\circ$ ) the beam hit he mirror M1. ....	11
<b>Figure 9</b> On the left The Diffraction Encircled energy; on the right the RMS spot size Vs the field for the three Wave length. The black line represent the diffraction limit. ....	13
<b>Figure 10</b> On the left the footprint on the LCVR face, all the fields converge on the same area; on the right the spots on the focal plane. The scale is 1 pixels (18 $\mu\text{m}$ ) . ....	13
<b>Figure 11</b> The 2 Baseline and Back designs. ....	14
<b>Figure 12</b> On the left the diffraction encircled energy show how more than the 80% of the fields is enclosed into two pixel; on the right RMS spot size Vs Filed show that after $1.5^\circ$ FoV the system is diffraction limited. ....	15
<b>Figure 13</b> The spots in the image plane, the scale is 1 pixel. ....	15
<b>Figure 14</b> Baseline and Back designs .The size of the designs is equivalent. ....	15

## Visible-light path and polarimeter

METIS will study the solar corona in the Visible Light (VL) band 500 – 600 nm and in two narrow band in the UV at 30 nm and 122 nm. The two focal planes of the instrument are displayed in Figure.1. An interferometric filter will act both as folding mirrors as filter.

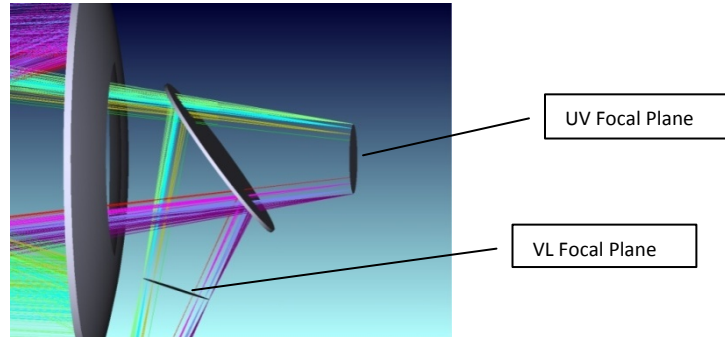


**Figure 1** The 2 focal planes UV and VL of METIS

The VL channel will hold an LCVR (Liquid Crystal Variable Retarder) so it is needed a relay system to collimate the beam before the LCVR and focalize the beam outgoing from LCVR on the CCD camera. In Table 1 are summarized the main requirements for this device and the project status. It has been developed also a backup design using a motorized QW plate instead the LCVR. In this case there are no problems of incidence angle and the design is in general freer but mountings could involve the design because the presence of a motor needed to rotate the QW plate.

	Required	VL path ver. 01
Diameter	25,4 mm<D<40 mm	25,4 mm
Acceptance angle	<3°	3,4°
Collimation	yes	yes
Circular footprint	yes	yes

*Table 1* The main constrains for the relay system optical design, “circular footprint” mean that on the LCVR face the coming image from the telescope must be circular not annular, in this way all the fields are concentrated in the same area of the LCVR.

## Constrains

Constrains in METIS VL path come from several sides: LCVR needs an input collimated beam and has an acceptance angle of  $\pm 3^\circ$ , on the other side METIS telescope is rather fast (300 mm focal length) furthermore METIS envelope is of small size so, to collimate the beam in a so little angle, we need optics with high dioptric power and this leads to the use of many glasses to minimize chromatic aberrations. Here the choice of adequate glasses is limited by the use of radiation hardness glasses. In addition there is the Polarimetric noise introduce by the folding mirror that depends from the incidence angle. All those problems will be discussed in next paragraph suggesting suitable solutions.

## Physical Limit

The Lagrange invariant is an important constrains to the system. Let the height of the paraxial marginal ray be  $y_M$  at the entrance pupil and  $y'_M$  at the exit pupil, and that of the paraxial chief ray by  $y_C$ , at the object plane and  $y'_C$  at the image plane, Figure 2. Let the angles of these rays be  $u_M$ ,  $u_C$ ,  $u'_M$ ,  $u'_C$ . The two-ray paraxial invariant is

$$L = ny_M u_C = n' y'_M u'_C \quad \text{eq.1}$$

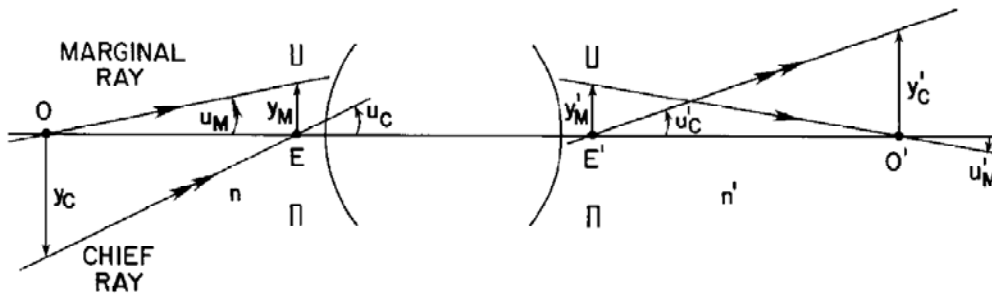


**Figure 2** Schematic diagram of a lens with object and image planes, entrance and exit pupils, and marginal and chief rays. The entrance pupil is located at E and the exit pupil at E'. The chief ray passes through the edges of the fields and the centers of the pupils. The marginal ray passes through the axial object and image points and the edges of the pupils (from Handbook of Optics, McGraw-Hill)

Now at the entrance pupil, the front aperture of the coronagraph, the incoming beam is collimated because coming from infinite and  $y_M = 20 \text{ mm}$  and  $u_C = 3^\circ$ . This means that wherever in the optical system it is needed re-collimate the beam into an angle of  $\pm 3^\circ$  the diameter of the beam will be 40 mm to save the Lagrange Invariant. This concept is linked to the conservation of the system etendue that is saved for ideal systems but this is a real system so the expected limit for the diameter of the LCVR is  $>40 \text{ mm}$ .

Looking at eq. 1, there is also the dependence from the refractive index so the invariance could be saved increasing it. For the LCVR system this could be translated in the presence of a glass window in contact with the LCVR. The index of refraction of this glass can be roughly calculated with eq. 1 i.e. for  $y'_M = 1/2 \text{ inch}$  inch:

$$n' = 1 * 20 * 0.052 / 12.5 * 0.052 = y_M / y'_M = 1.6 \quad \text{eq.2}$$

in the ideal case. ZEMAX simulation using a real radiation hard glass applied to the real system needs a SF6G05 glass with a refraction index of 1.81.

### LCVR Polarimeter Constrains

LCVR polarimeter device is composed by 5 elements (Figure 3)

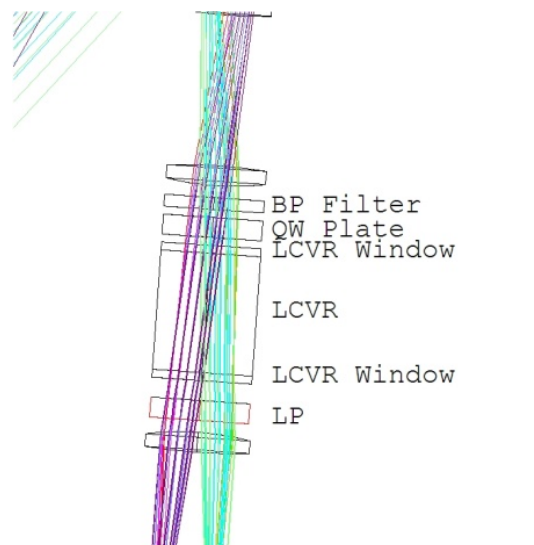


**Figure 3** The LCVR devices and its parts, the ray comes from the farer fields at  $\pm 3^\circ$  and are collimated in a cone of  $\pm 3^\circ$

1. The Band Pass filter usually is a flat borosilicate glass;
2. The Quarter Wave retarder is a birefringent element;
3. The LCVR window is SF6G05 glass;
4. The LCVR is the Achromatic Liquid Crystal Variable Retarder. 2 liquid crystals cells are contained into 2 layers of fused silica glass, or in SF57 flint glass;

5. The Linear Polarizer is the analyzer, typically a flat birefringent glass with BK7 windows.

### Acceptance angle

The main constrain is the acceptance angle of  $\pm 3^\circ$  and its implication to the system are explained in previous paragraph.

### Footprint

This second constrain is linked to the response uniformity of a liquid crystal media. This suggest to keep all the field in a spot as small as possible, this is in contrast with the Lagrange invariant if the incident angle for the collimated beam is  $\pm 3^\circ$ . The idea is so to stretch the beam to do this it is useful first to increase the focal length with a negative lens, after that a positive lens is needed to collimate the beam (Figure. 4).

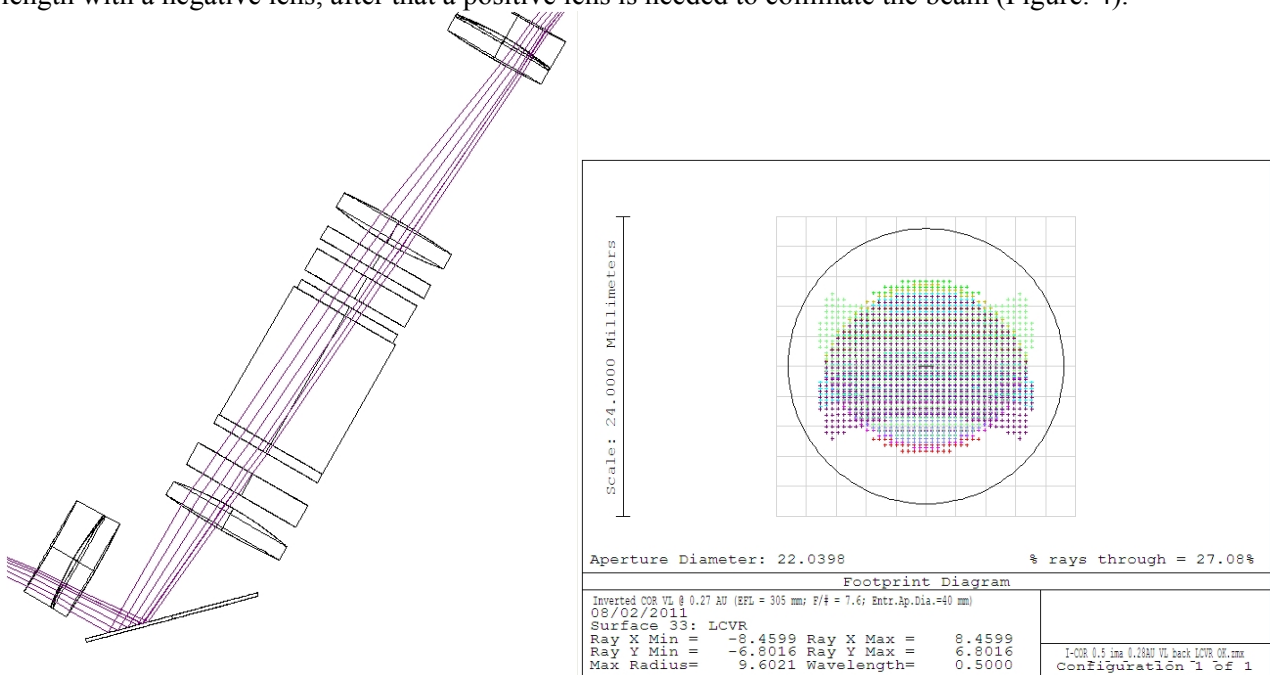


**Figure 4** On the left (a) the first part of the VL path, the beam is “stretched” to create on the LCVR plane (b) a superposition of all the fields to minimize effects due to a non uniformity in the LC.

### VL folding mirror “instrument polarization”

The instrumental polarization is the polarization noise ( $P_n$ ) introduced in the VL path by the folding mirror (FM), propagated through the devices and detected. The polarization noise depends in first analysis by the difference of the reflection indexes  $R_s$ ,  $R_p$  that for a specific material is depending from the incidence angle (and the wavelength). The resultant effect is that the beam after the reflection has a partial polarization in the planes S and P, furthermore this effect introduces also a phase difference between the two polarization planes that change the polarization state (i.e. from linear to elliptic). The polarimetric noise can be evaluated as the difference between the two indexes normalized to the sum of the indexes:

$$P_n = \frac{R_S - R_P}{R_S + R_P} \quad \text{eq.3}$$

In this case if  $R_S = R_P$   $P_n=0$  and no noise is present. For METIS VL path the requirement is a “instrument polarization”  $P_n < 0.01$  with a goal  $P_n < 0.005$ .

The two reflection coefficients depends on the complex refractive index and on the incidence angle in a different way for various material. In example in Tab. 2 Are listed the values for Aluminum (Al) and Magnesium Fluoride (MgF2) that will be used for the FM in METIS VL path. The indexes are for an incidence angle of  $45^\circ$ .



The FM layers structure seen by the VL is a layer of MgF2 over the Al layer, so to evaluate the  $P_n$  index, it is needed to make the sum weighted over the mean reflectivity of the 2 different parts.

	$R_s$	$R_p$	$P_n$	$F_s$ (deg)	$F_p$ (deg)	$F_s-F_p$
Al	0,94200	0,8874	0,029	-166,98	-153,95	-13,025
MgF2	0,06376	0,00406	0,880	180	180	0

Table 2 In the first 2 columns the Fresnell reflection coefficient for the 2 polarization planes S and P in the case of 45° reflection, on the third column the index  $P_n$ , on the last columns the phase shift. On the rows the materials used in FM. (values from Handbook of Optics, McGraw-Hill)

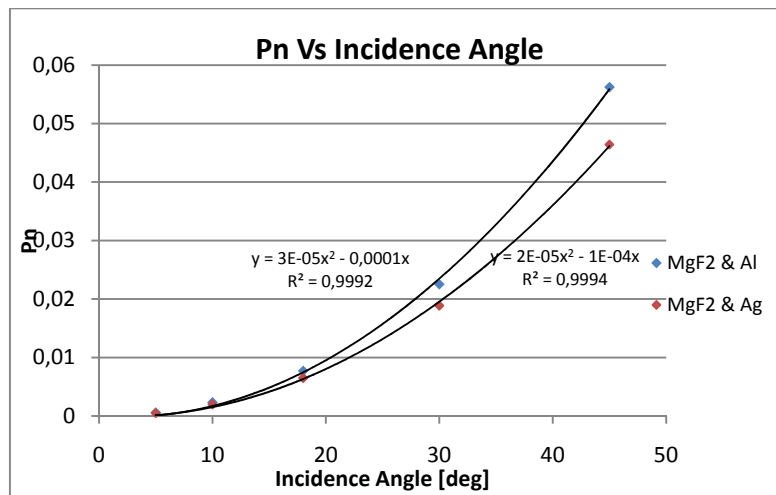
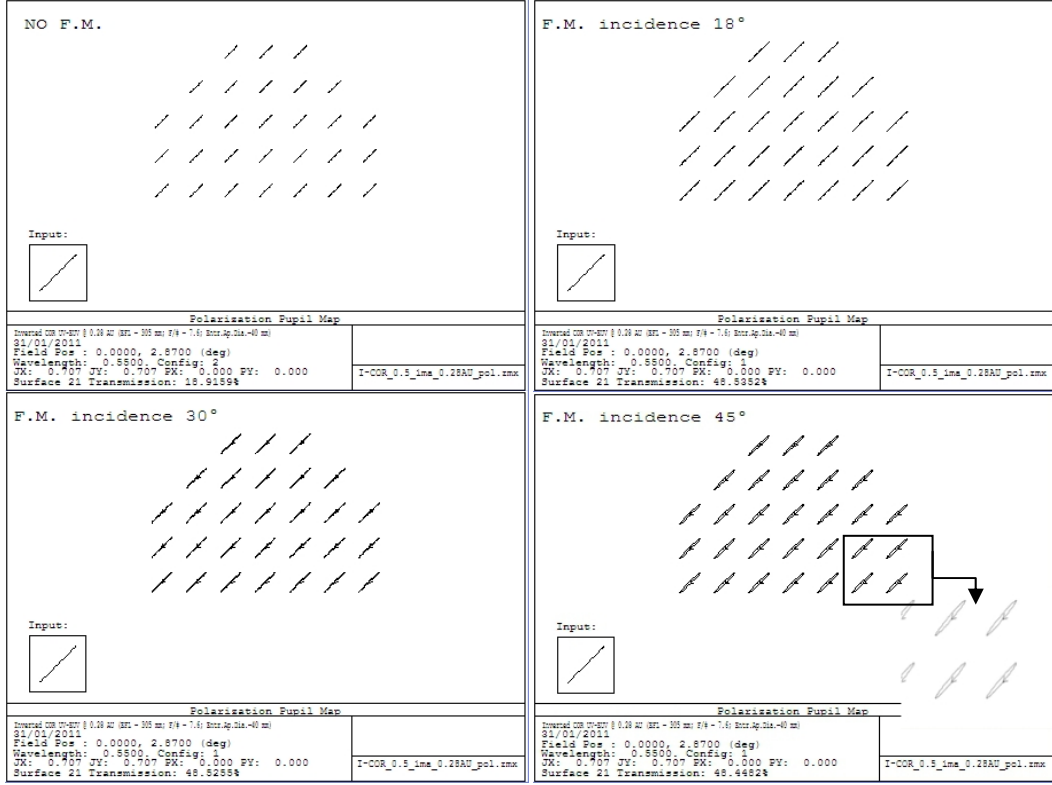


Figure 5 The blue dots represents the polarization introduce by a multi layer MgF2 & Al folding mirror in function of the incidence angle, the red dots for MgF2 and Ag. The lines are the fits relative to the two series, the relation is quadratic.

To improve VL path polarimetric performances it is needed either change coatings or change incidence angle. In Figure 5 is plotted the index  $P_n$  for some angles, a parabola well fit data so the result is that the relation between angle and instrumental polarization is quadratic. In particular to go under 0,01 (the 1% of polarization introduced by the FM), the angle should be under 20° now there is a problem of compatibility with the structure of METIS indeed the only allowed angles are over 30° and under 18°, but this point will be clarify in next chapter. In the plot is present a second curve relative to the Ag but the use of a different metal for FM is not so relevant because going to little angles the difference between Al and Ag is negligible i.e. for 18° incidence  $P_n(\text{Al})=0.0077$   $P_n(\text{Ag})=0.0065$ .

### Cross-Talk Polarization

In addition to the effect due to the difference between the reflection coefficient in S and P planes FM can introduce also a phase shift and the final effect can be the change in polarization state known as cross talk polarization from linear to elliptical. This effect can be appreciable if the input light is linear polarized as we expect is the light from the solar K-corona. This effect has been confirmed by a ZEMAX simulation. The FM is coated by aluminum, a beam polarized L+45 is introduced in the telescope and the polarization pupil map in the telescope VL focal plane is displays the polarization state for the field up to +3° (Figure 6). As expected if there is no FM the polarization state is the same from the entrance pupil up to the focal plane. When the FM is introduced into the optical path the polarization state change and the increasing in phase difference between S and P polarization planes leads to an elliptical polarization (Tab. 3).



**Figure 6** ZEMAX polarization pupil maps in the METIS VL focal plane. The boxes are for 3 position of the FM . In the last (bottom dx corner) a zoom show the visible change in polarization state.

Now the Stock vector for a L+45 input polarized beam is  $S_{in}$  the Mueller matrix for a non polarizing filter is  $M_{id}$  in the case of no polarization introduced by FM  $S_{out}=S_{in}$  (eq.4).

$$S_{in} = \begin{pmatrix} 1 \\ 0 \\ 1 \\ 0 \end{pmatrix} \quad M_{id} = \begin{pmatrix} 1000 \\ 0100 \\ 0010 \\ 0001 \end{pmatrix} \quad S_{out} = M_{id} \cdot S_{in} \quad \text{eq.4}$$

But in the case in exam a phase shift  $\varphi=\varphi_s - \varphi_p$  is introduced between the 2 components of the electric field, so the FM acts as a “retarder”. In this case the Mueller matrix change and also  $S_{out}$  :

$$M_{ret} = \begin{pmatrix} 1 & 0 & 0 & 0 \\ 0 & 1 & 0 & 0 \\ 0 & 0 & \cos \varphi & -\sin \varphi \\ 0 & 0 & \sin \varphi & \cos \varphi \end{pmatrix} \quad S_{out} = \begin{pmatrix} 1 \\ 0 \\ \cos \varphi \\ \sin \varphi \end{pmatrix} = M_{ret} \cdot S_{in} \quad \text{eq. 5}$$

In the case of no phase shift introduced  $\varphi=0$  and the previous case is verified. So the polarization cross-talk is a change of value between the 2 Stocks vector elements  $S_2$  an  $S_3$ , while the total polarized intensity is saved by the relation

$$I_{pol} = \sqrt{S_1^2 + S_2^2 + S_3^2} \Rightarrow 1 = \sqrt{\cos^2 \varphi + \sin^2 \varphi} \quad \text{eq. 6}$$

A parameter to evaluate the cross-talk linear polarization can be:

$$P_{CT} = S_{2IN} - S_{2OUT} = 1 - \cos \varphi \cong \frac{\varphi^2}{2} \quad \text{eq. 7}$$

Where in eq.7 the cosine is approximated for little phase shift in Maclaurin series stopped at the first term and the phase is in radians.

Incidence (deg)	$\varphi_s$ (deg)	$\varphi_p$ (deg)	$\varphi=\varphi_s - \varphi_p$	$P_{CT}$
18°	-162°,45	-160°,59	-1°,866	0,0005
30°	-164°,03	-158°,68	-5°,352	0,0044
45°	-166°,98	-153°,95	-13°,025	0,0258

**Table 3** The phase shift in the two S and P polarization planes Vs the incidence angle.

The scientific goal gives us a constrain in  $P_{CT} < 0,01$  with a goal at  $P_{CT} < 0,005$ . From Tab.3 now is clear as a  $45^\circ$  FM introduce a cross-talk polarization out of our constrains but in this case a  $30^\circ$  FM could be an acceptable solution even if to minimize this effect  $18^\circ$  FM seems to be the optimal solution.

## Envelope

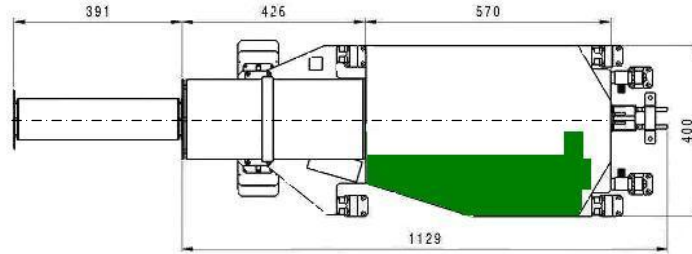


**Figure 7** A draw of METIS envelope, the green area represents the space for the VL path location.

In figure 7 METIS's envelope, the green area (just to have a roughly idea) is the part of the envelope that will hold the VL path and the LCVR. The distance between the axis (dash and dotted line) and lower part of the envelope is 230 mm.

## Glass

Glasses used in the design are radiation hardness from the SHOTT catalogue. RH glasses are Cerium doped glasses resistant to the discoloration by  $\gamma$ -rays, electron and proton bombardment. Glasses user are:

Glass	n	$V_d$
SF6G05	1.81	25.3
LAK9G15	1.69	54.74
BK7G18	1.52	63.6

*Table 4* Glasses used in VL path, the refraction index ( $n$ ) and the Abbe number ( $V_d$ )

## Mass budget

The mass budget of the optics is divided in 2 parts. The first regarding the VL path with the LCVR, the second with a motorize QW plate instead the LCVR. All the masses are calculated without to take in account the mechanical mounts and the FMs.

Element	Material	Volume cc	Density g/cc	Mass g
In doublet I <sub>st</sub> glass	SF6G05	1.788	5.200	9.299
In doublet II <sub>nd</sub> glass	LAK9G15	1.391	3.525	4.905
Collimating Lens	BK7G18	2.082	2.520	5.247
BP filter	BK10	1.472	2.390	3.519
QW	Calcite	2.454	2.711	6.653
LCVR Window	SF6G05	0.981	5.200	5.105
LCVR	BK7	14.726	2.510	36.962
LCVR Window	SF6G05	0.981	5.200	5.105
LP	Calcite	2.454	2.711	6.653
Collimating Lens	BK7G18	2.082	2.520	5.247
Out doublet I <sub>st</sub> glass	LAK9G15	2.016	3.525	7.108
Out doublet II <sub>nd</sub> glass	SG6G05	2.986	5.200	15.532

**LCVR case total mass: 111.340**

*Table 5* The elements in the VL path for the LCVR case.

Element	Material	Volume cc	Density g/cc	Mass g
Lens	SFG05	2.700288	5.200000	14.041497
Doublet I <sup>st</sup> glass	K5G20	1.956034	2.593000	5.071995
Doublet II <sup>nd</sup> glass	BK7G18	2.587301	2.520000	6.519999
BP filter	BK10	1.472622	2.390000	3.519566
QW	Calcite	2.454369	2.711000	6.653795
QW	Calcite	2.454369	2.510000	6.160467
LP	Calcite	2.454369	2.711000	6.653795
Doublet II <sup>nd</sup> glass	BK7G18	2.587301	2.520000	6.519999
Doublet I <sup>st</sup> glass	K5G20	1.956034	2.593000	5.071995
Lens	SFG05	2.700288	5.200000	14.041497

**QW case total mass: 74.489 g**

*Table 6 The elements in the VL path for the QW case.*

The QW case looks more light then the LCVR case: 37 g less mass however in this budget are not included the mechanical parts and the QW needs also a motor to be rotated so the final mass of the QW case could be more elevated then the LCVR case.

## Optical performances

For the considerations made in the previous chapter regarding the instrumental polarization and the cross-talk polarization, one critical point of the design is the interception angle between the optical axis of the telescope and the FM. From previous considerations it is clear that 45° FM introduces too much polarization noise so 2 angles were advanced: 18° and 30°. The reason for the choice of such angles is clear from Figure 8: in the range between 18° and 30° the reflected beam hits M1; over 30° is behind M1 but down 18° the beam cross the hole of M1 and it is back reflected into the telescope. Indeed this last region is quite small almost 16°.5-18° because down from 16°.5 the collimation optics enters in the FoV of the telescope.

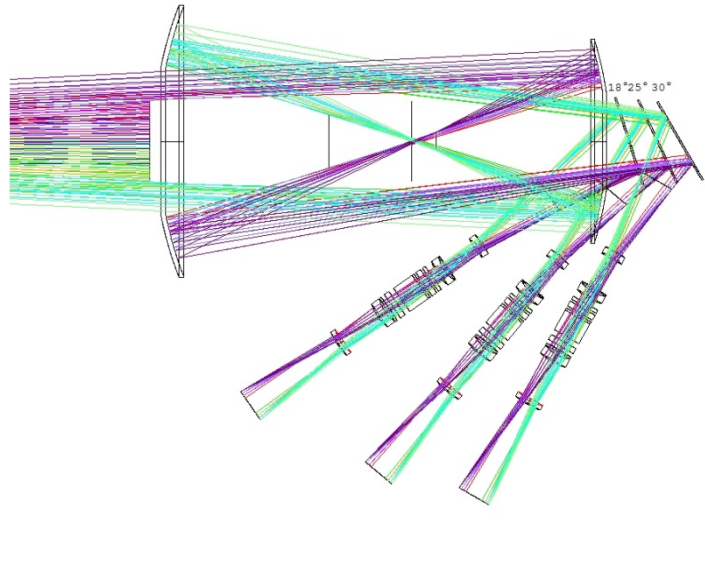


**Figure 8** Comparison between different FM angles. In the range between 30° and 18° (i.e. 25°) the beam hit the mirror M1.

In the following the design with the FM angle  $\geq 30^\circ$  will be called **Baseline VL Path** design, the one with the FM angle  $\leq 18^\circ$  **Back VL Path**.

The designs presented are:

	Baseline	Back
LCVR	Yes	Yes
Motorized QW	Yes	Yes

Table 7

For all that cases the system will be optimized trying to optimize RMS spot size compatibly considering all the constrains explained up to now.

### LCVR design

The idea for this design is to collimate the beam stretching it with a negative doublet. After that a positive lens collimates the beam into the LCVR device. After the LCVR device the same two lenses inverted focus the beam on the image plane.

#### SURFACE DATA SUMMARY:

Radius	Thickness	Glass	Diameter	Conic	Name
Infinity	-68.33445		30.63066	0	<b>VL Focal Plane</b>
123.2624	-5	SF6G05	20	0	<b>Doublet</b>
-51.40329	0		20	0	
-82.2608	-5	LAK9G15	20	0	
94.37943	-41.9213		20	0	
75.86701	-3		25	0	<b>Collimation Lens</b>
Infinity	-3	BK10	25	0	<b>BP filter</b>
Infinity	-2		25	0	
Infinity	-5	CALCITE	25	0	<b>QW</b>
Infinity	-2		25	0	
Infinity	-2	SF6G05	25	0	<b>LCVR Win</b>
Infinity	-30	BK7	25	0	<b>LCVR</b>
Infinity	-2	SF6G05	25	0	<b>LCVR Win</b>
Infinity	-5		25	0	
Infinity	-5	CALCITE	25	0	<b>LP</b>
Infinity	-3		25	0	
-75.86701	-5	BK7G18	25	0	<b>Collimation Lens</b>
162.222	-42.47447		25	0	
-94.37943	-5	LAK9G15	25	0	<b>Doublet</b>
82.2608	0		25	0	
51.40329	-5	SF6G05	25	0	
-123.2624	-25		25	0	
Infinity	43.334	MIRROR	47.38076	0	<b>F.M.</b>
Infinity			30.78211	0	<b>Image Plane</b>

Table 8 All the parameter of LCVR VL path optics

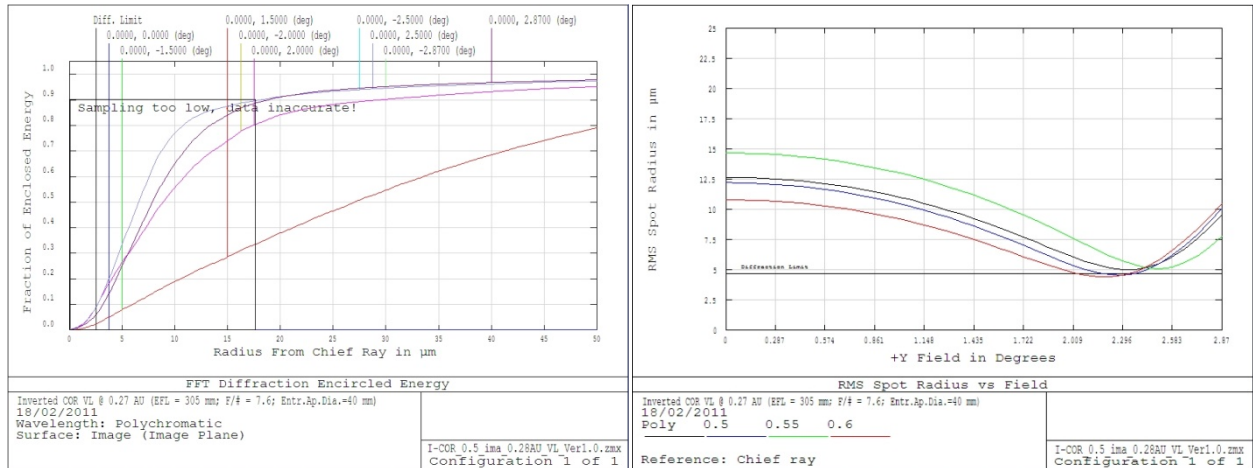


**Figure 9** On the left The Diffraction Encircled energy; on the right the RMS spot size Vs the field for the three Wave length. The black line represent the diffraction limit.

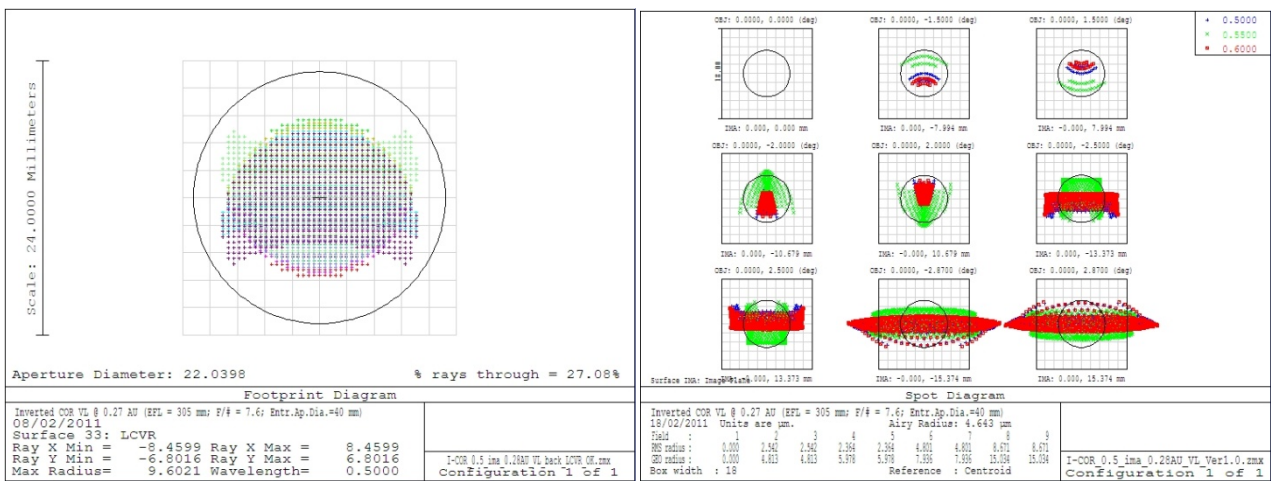


**Figure 10** On the left the footprint on the LCVR face, all the fields converge on the same area; on the right the spots on the focal plane. The scale is 1 pixels (18  $\mu\text{m}$ ).

The requirements of concentration of the footprint on the LCVR front face and incidence angle are satisfied but the Diffraction Encircled Energy and the spot size are still not optimized indeed the system need to be bettered of a factor 2.

### Baseline Vs BackVL Path

In Figure. 11 the system in the 2 version Baseline and Back. Maximum extension in the y direction is 220 mm for Baseline case and 202 mm for Back case both are compatible with the envelope. Up to now the x direction (the one normal to the draw) is not used, it could be implemented to adjust to the envelope.

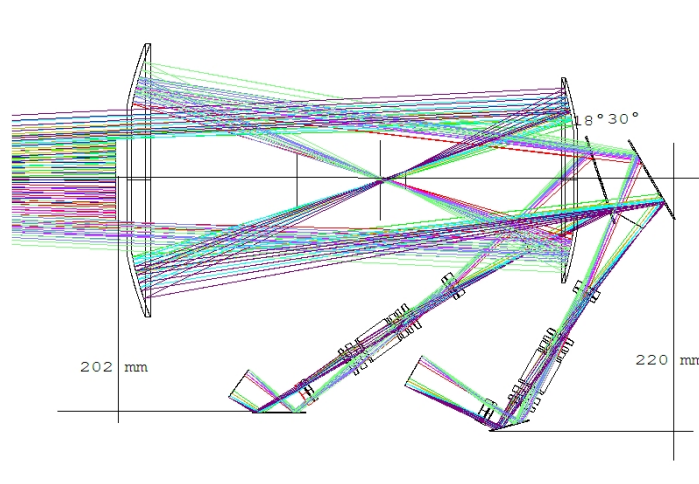


**Figure 11** The 2 Baseline and Back designs.

The optical system is build to use the same lenses for both the baseline and back cases so the performances of this case are the same of the previous.

### Back up HW design

As before the design has been developed for the 2 case baseline and back VL path and the optics are the same for the 2 case so optical performances do not change. In this case, the absences of constrains in the beam incidence gives more freedom to the design. The collimation lenses before the polarimeter are the same as the lenses after the polarimeter. The performances of the system are diffraction limited: Strehl Ratio is > 0.94.

Element	Material	Radius	Thickness	Semi Diameter
Lens I <sup>st</sup> Surf	SFG05	-44.223	5	12.5
Lens II <sup>nd</sup> Surf		-26.487	4.369	12.5
Doublet I <sup>st</sup> Surf	K5G20	-31.492	3.645	12.5
Doublet II <sup>nd</sup> Surf		129.587	0	12.5
Doublet III <sup>rd</sup> Surf	BK7G18	129.587	7	12.5
Doublet IV <sup>th</sup> Surf		121.281	5	12.5
BP filter	BK10	$\infty$	3	12.5
		$\infty$	2	12.5
QW	Calcite	$\infty$	5	12.5
		$\infty$	7	12.5
QW	Calcite	$\infty$	5	12.5
		$\infty$	7	12.5
LP	Calcite	$\infty$	5	12.5
		$\infty$	5	12.5
Doublet IV <sup>th</sup> Surf	BK7G18	121.281	7	12.5
Doublet III <sup>rd</sup> Surf		129.587	0	12.5
Doublet II <sup>nd</sup> Surf	K5G20	129.587	-3.645	12.5
Doublet I <sup>st</sup> Surf		-31.492	4.369	12.5
Lens II <sup>nd</sup> Surf	SFG05	-26.487	5	12.5
Lens I <sup>st</sup> Surf		-44.223	88.552	12.5

*Table 9 All the parameter of HW VL path optics*

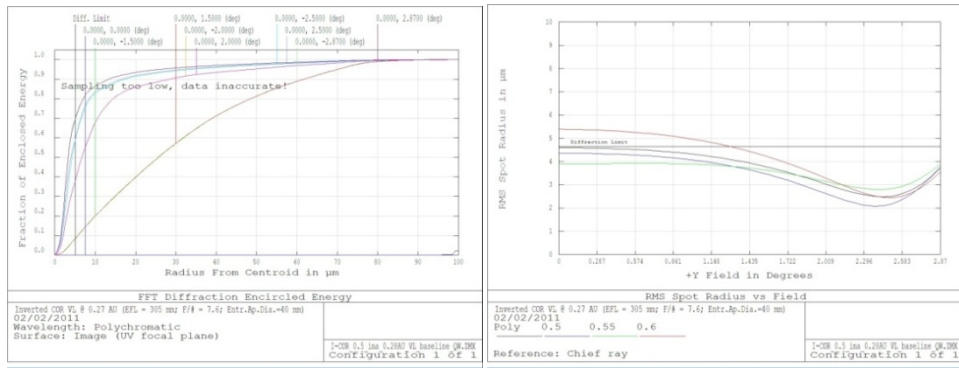


**Figure 12** On the left the diffraction encircled energy show how more than the 80% of the fields is enclosed into two pixel; on the right RMS spot size Vs Filed show that after 1.5° FoV the system is diffraction limited.

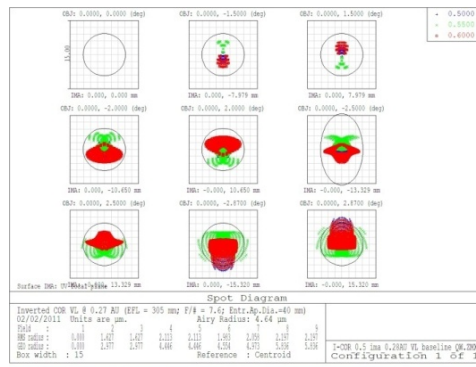


**Figure 13** The spots in the image plane, the scale is 1 pixel.

### Baseline Vs Back VL Path

In this case the compactness of the polarimeter reduces the dimension of the system. The maximum elongation on the y axis is 202 mm. Again one remark is the presences of a motor to rotate the HW central element. The introduction of this element could increase the dimension of all the system.

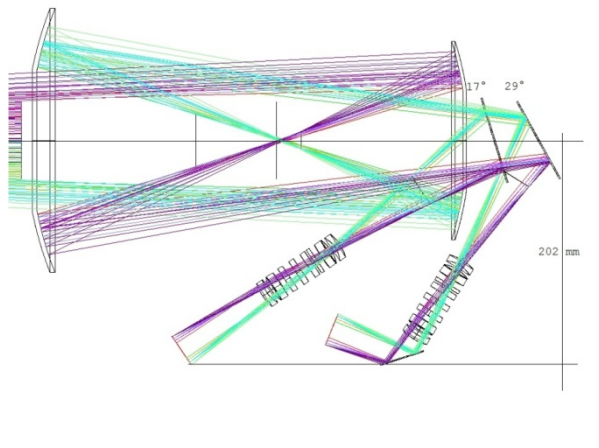


**Figure 14** Baseline and Back designs .The size of the designs is equivalent.



## List of Acronyms

EO: External Occulter  
EP: Entrance Pupil  
FA: Front Aperture  
LCVR: Liquid Crystal Variable Retarder  
MA : Mechanical Axis  
METIS: Multi Element Telescope for Imaging and Spectroscopy  
SCORE: Sounding – Rocket Coronagraph Experiment  
VL: Visible Light

## References

- [1] *Inverted-COR: Inverted –Occultation Coronagraph for Solar Orbiter*, OATo Technical Report Nr 119  
Date 19-05-2009, Silvano Fineschi;
- [2] *Stray light Analysis of Reflecting of a UV Coronagraph/Polarimeter with Multilayer Optics*; S. Fineschi,  
M. Romoli, R.B. Hoover, P.C. Baker, M. Zukic, J. Kim, A.B.C. Walker Jr; SPIE Vol. 2010 X-Ray and  
Ultraviolet Polarimetry (1993);
- [3] *Experimental study of external occulter for the Large Angle and Spectrometric Coronagraph 2:LASCO-  
C2*; M. Bout, P. Lamy, A. Maucherat, C. Colin, A. Llebaria; 1 Aug. 2000, Vol.39 No. 22, Applied Optics.
- [4] *Stray light analysis for the SCORE coronagraph of the Herschel mission*; Federico Landini, PhD Thesis  
in Astronomy, Università degli Studi di Firenze;
- [5] Smith, Modern Optical Engineering, Mc Grow Hill